

## MICROALGAE AS NATIVE OXYGEN SUPPLIERS IN BICAMERAL MICROBIAL FUEL CELLS

A. CUCU<sup>a</sup>, T.A. COSTACHE<sup>a</sup>, A. TILIAKOS<sup>a</sup>, I. STAMATIN<sup>a,\*</sup>, A. CIOCANEA<sup>b</sup>

<sup>a</sup> *University of Bucharest, Faculty of Physics, 3Nano-SAE Research Centre, Bucharest-Magurele, Romania*

<sup>b</sup> *Politehnica University of Bucharest, Energetic Dep., Bucharest, Romania*

The present study introduces microalgae as native oxygen suppliers in bicameral microbial fuel cells, thus proposing an alternative solution to the oxygen-reduction reaction-chain issue. An MFC experimental prototype that employs a *Saccharomyces cerevisiae* monoculture in the bioanode is tested for three different catholytes: a phosphate buffer solution, a buffer solution with an oxidizing mediator (20mM  $K_3Fe(CN)_6$ ) and a solution hosting a microalgal culture. The microalgae MFC presents a comparable electrochemical response to the ferrocyanide mediator system, reaching power densities of  $\sim 118mW/m^2$  around the current density level of  $700mA/m^2$  and a maximum in generated potential of  $\sim 520mV$ . However, microalgae MFCs display a more stable electrochemical response over time (with faster acclimation times, smoother transitions into lower production levels and a higher average performance throughout operation), benefitting from the constant oxygen supply provided by microalgal photosynthesis at the cathode. Thus, the use of microalgae as oxygen suppliers in MFC cathodes presents a cost-effective, sustainable and power-efficient alternative to the use of toxic chemical mediators, giving reasonable ground to suggest coupling microalgae MFCs to wastewater treatment processes.

(Received July 25, 2013; Accepted September 27, 2013)

*Keywords:* Microbial fuel cell, cathode catalysts, microalgae, power performance

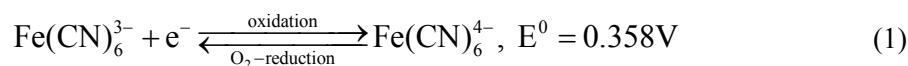
### 1. Introduction

In the past decade, microbial fuel cells (MFCs) have received considerable interest as a promising new technology allowing for simultaneous electricity generation and water treatment [1, 2]. Improvements in design (e.g. architecture, materials) seeking to augment generated power densities have not managed, however, to counteract the inherent limitations originating from cathodic oxygen reduction reactions (ORR); these are sluggish and require an excess of dissolved oxygen (DO), provided traditionally by air bubbling at the cathode chamber, thus increasing energy costs and reducing overall efficiencies. Another limitation hindering wide-scale implementation lies in high-efficiency (and high-cost) precious metals (e.g. Platinum) used as catalytic coatings in cathode materials; wastewater media rapidly poison such materials, thus imposing the need for their frequent replacement.

Mediators acting as terminal electron acceptors in the cathode have a positive effect on MFC power generation [16]. The highest power output obtained by a system using a potassium ferrocyanide mediator reached  $258W/m^3$  in a 6-unit stacked MFC, with graphite granules as electrodes and a 50mM concentration of hexacyanoferrate ( $Fe(CN)_6^{3-}$ ) in buffer solution [2-4]; essentially, mediators such as hexacyanoferrate lower the required oxidation potential for reoxidation [5, 6], according to:

---

\* Corresponding author: [istarom@3nanosae.org](mailto:istarom@3nanosae.org)



The reoxidation of hexacyanoferrate(II) requires an excess of oxygen and regular replenishment [7]; the latter classifies ferrocyanide mediators as unsustainable alternatives, even though they reach performances comparable to Pt catalysts [2, 3, 8].

Researches into non-precious metal cathode catalysts and chemical modifications to air cathodes have provided considerable advances in these areas, although there is still room for improvements in cathode stabilization and power performance: bicameral MFCs require catholyte aeration, which translates into power consumption, either from the MFC itself or from external sources, thus reducing overall efficiency [6, 9].

Microalgae as native oxygen suppliers may provide an interesting alternative that combines oxygen production in the cathodic chamber and removal (i.e. reduction) of pollutants (e.g. nitrate) that appear frequently in agricultural and domestic wastewaters [1]. Oxygen results as a product of microalgal photosynthesis [10, 11]; cultures of microalgae may be employed to counter DO depletion in the catholyte, thus improving MFC power performance by stabilizing DO levels [17]. In combination with nitrate reduction, microalgae may act as electron acceptors (i.e. mediators) in the cathode, covering the potential window from oxygen ( $E^0=+820\text{mV}$ ) and nitrate ( $E^0=+430\text{mV}$ ) [11, 12].

Based on the above, we have assembled an MFC experimental prototype that employs microalgae in the cathode and a *Saccharomyces cerevisiae* monoculture in the bioanode. *S. cerevisiae* is a non-pathogenic microbial species that offers facile mass cultivation and excellent maintenance, being capable of remaining in dry state for long time periods [13, 14]. Recent investigations in MFCs using said microbial species yielded power densities ranging from  $2.19\text{mW}/\text{m}^2$  (bicameral MFC using graphite electrodes and methylene blue as mediator) [8] and  $3.1\text{mW}/\text{m}^2$  (monocameral MFC using carbon paper electrodes and Pt as catalyst) [13] to  $500\text{mW}/\text{m}^2$  (stacked MFCs in continuous operating mode using graphite electrodes, neutral red as mediator and potassium permanganate as oxidizing agent) [14]. In this prototype, we have employed carbon paper as electrodes and tested its performance for three different catholytes: a phosphate buffer solution, a buffer solution with an oxidizing mediator (20mM  $\text{K}_3\text{Fe}(\text{CN})_6$ ) and a microalgal culture.

## 2. Materials and methods

### 2.1 Materials

The following materials were used in the assembly and operation of the MFCs:

*Anolyte solution:* 1.5g dried culture of *S. cerevisiae* (Pakmaya), activated in 150ml sterile medium (0.75g glucose, 0.6g malt extract and 1.2g  $\text{NaH}_2\text{PO}_4$ ) for 1h at  $30^\circ\text{C}$  with continuous stirring.

*Catholyte solutions:* Phosphate buffer solution. Potassium ferrocyanide ( $\text{K}_4\text{Fe}(\text{CN})_6$ ), used as received, for a catholyte solution of 20mM ferrocyanide oxygen-reducing mediator.

*Microalgal culture:* grown photoautotrophically in a flask containing 200ml standard medium (Allen and Arnon, PhytoTechnology Laboratories) [15]. The culture was illuminated using a simple desk lamp and kept under constant aeration using an air-pump (Hailea Group Ltd). After reaching the desired density, an aliquot of the algal culture was transferred to the cathode compartment of the MFC.

**Proton-exchange membrane (PEM):** (Nafion 117, DuPont) PEM was activated by boiling in  $\text{H}_2\text{O}_2$  (3% v/v) for 2h, then in  $\text{H}_2\text{SO}_4$  (0.5M) for 2h and finally in DI water for 2h and stored in DI water before use.

**Electrodes:** carbon paper (Ballard Carbon Paper, Sainergy Fuel Cell India Ltd.), cleaned and activated in nitro-hydrochloric acid (1:3 vol. mixture of concentrated nitric acid and hydrochloric acid) for 2h, washed with DI water and dried at  $70^\circ\text{C}$  before use.

## 2.2 Experimental setup

Three variations of the bicameral system were assembled based on different catholytes, with the two compartments separated by a PEM: the first system contained a phosphate buffer solution, the second a buffer solution with 20mM potassium ferrocyanide and the third the microalgal culture (Fig. 1). Carbon paper was used as electrode material for both compartments, with a surface area of  $24\text{cm}^2$ ; the electrodes were connected to an acquisition plate; the distance between electrodes was 7cm. The cathodic compartment had a volume of 150ml and contained the catholyte solutions; the anodic compartment had a volume of 150ml and contained a monoculture of *S. cerevisiae* as biocatalyst.

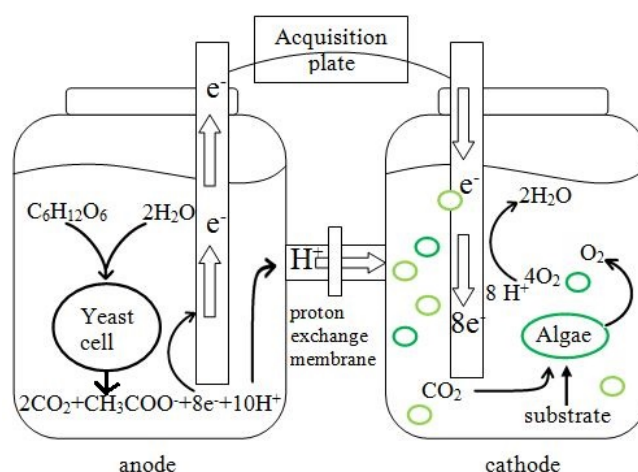


Fig. 1: Experimental microalgae MFC setup, with *S. Cerevisiae* at the anode and microalgae at the cathode.

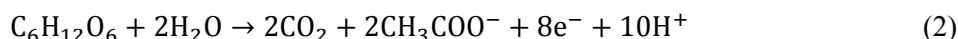
## 2.3 Analytical techniques

Conductivity ( $\sigma$ ), pH and dissolved oxygen (DO) for both compartments were measured every 24h using Thermo Scientific Orion 5-Star Benchtop Meter with the afferent electrodes. Electric potential output was measured using a Picotech ADC 10/11 data acquisition unit; all systems were monitored at room temperature every 5 minutes for 5 days.

Polarization and power density curves were obtained by varying the external resistance in a decreasing order at 15min intervals at each step. Current density was calculated from  $I = E/RA$ , where  $E$  is the cell voltage (V),  $R$  is the external resistance ( $\Omega$ ), and  $A$  is the projected surface area of the cathode ( $24\text{cm}^2$ ). Power density was calculated using  $P = IE/A$ .

Cyclic voltammetry was conducted in both chambers by using a Voltalab 401 system to examine the electrochemical behavior of the MFCs, to determine the double layer capacity ( $C_{DL}$ ) of the bioelectrodes and to observe the redox activity in both chambers. The electrochemical analysis performed in each chamber employed the electrode from the opposite chamber as an auxiliary electrode, and a reference electrode (standard calomel electrode: SCE XR110) placed in the same chamber as the auxiliary one and close to the PEM.

All calculations were based on the chemical reaction for glucose fermentation [16]:



Coulombic efficiency  $E_C$  was calculated as the ratio of the measured total charge to the predetermined theoretical charge respective to the amount of glucose metabolized [16]:

$$E_C = \frac{C_{Ex}}{C_{th}} = \frac{M_s \int_0^t I dt}{F n_{ex} V_{an} \Delta c} \quad (3)$$

, where  $C_{Ex}$  is the total recovered charge, calculated by integrating the current measured at each time interval according to:

$$C_{Ex} = \sum_{i=1}^T (E_i t_i) / R \quad (4)$$

$C_{Th}$  is the total theoretical charge,  $M_s$  is the molar mass of the substratum,  $F$  is Faraday's constant,  $n_{ex}$  is the number of electrons exchanged per mole of substrate,  $V_{an}$  is the volume of liquid in the anode chamber,  $\Delta c$  is the substrate change in concentration and  $R$  is the external resistance. For our calculations, we have assumed the complete enzymatic (via maltase) hydrolysis of maltose contained in the malt extract into two glucose molecules per maltose molecule; this gives a total substrate mass of 1.382g and an initial concentration of 9.213g/L.

### 3. Results and discussion

#### 3.1 Electrochemical performance

Electric potential output for all system configurations has been measured continuously for 5 days in 5 minute intervals; the first day (24h) of measurements provided a clear picture of the acclimation behavior (Fig. 2), displaying marked differences between the times needed for the systems to reach their maximal potential values: the buffer-catholyte system reached its maximum output value of 518mV after roughly 6 hours after initiation, maintaining this value for less than 2 hours; the ferrocyanide system reached a maximum of 522mV after a much longer interval of roughly 15 hours, maintaining its peak performance for 8 hours; the microalgae system displayed an intermediate behavioral pattern, reaching its maximum value of 519mV after an 8 hour interval and maintaining it for about 6 hours.

Statistical analysis of the first 24 hours of acclimation times offers an insight into the behavioral patterns of the systems (Table 1): in all systems, modal values coincide with the respective maximal values, indicating the systems' tendency to arrive and settle at their peaks; however, mean values are considerably lower than the respective modes (mean $\pm$ SD: 0.49891 $\pm$ 0.01464V for the buffer system, 0.48945 $\pm$ 0.04741V for ferrocyanide and 0.49605 $\pm$ 0.02245V for microalgae), indicating the prominence of left tails in all frequency distributions, consistent with the observed acclimation times. This is more clearly displayed in the corresponding frequency histograms and box plots (Fig. 3): the buffer catholyte system has the shortest tail, with a higher frequency density around the mode (thus its higher mean and lower SD) indicating its faster acclimation time, but it does not settle in a single mode for long, displaying a gradual build-up of frequencies around the peak value; the ferrocyanide system displays the most abrupt acclimation behavior, with a long tail and frequencies at the low end (mean value lower than the median), indicating a longer acclimation time with a cascade of intermediate stages and a pronounced peak at the higher end; the microalgae system displays an intermediate behavior, with a pronounced peak but shorter tail, thus a smoother transition to its maximum value.

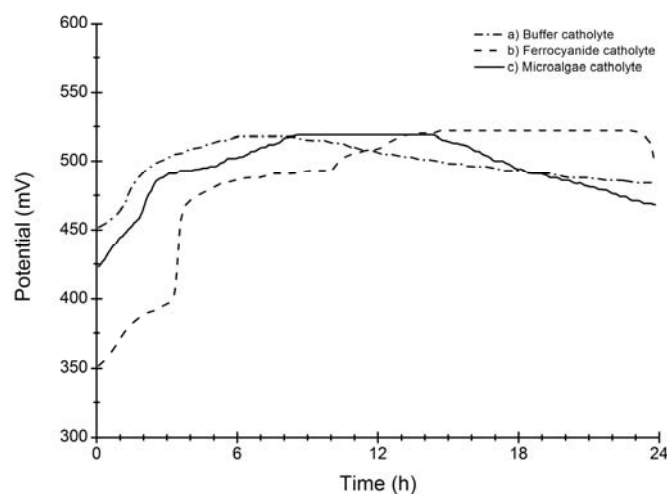


Fig. 2: Acclimation time (first 24h after system initiation) for all MFC configurations operated in batch mode. The buffer system (a) displays a smooth transition to its peak value of 518mV after an acclimation interval of 6h; the ferrocyanide system (b) reaches its peak value of 522mV after a 15h cascade of intermediate stages; the microalgae system (c) displays an intermediate behavior, reaching its peak value of 519mV after an 8h interval.

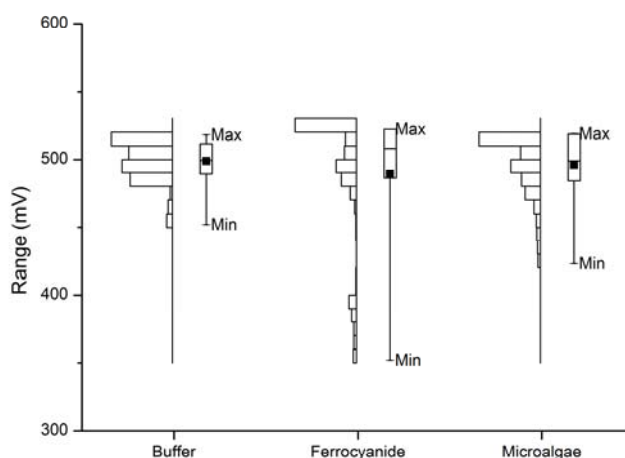


Fig. 3: Box plots and frequency histograms of the acclimation time for all MFC configurations. Solid squares indicate mean values; boxes display 1<sup>st</sup> (25%) quartiles (bottom side), median values (middle line) and 3<sup>rd</sup> (75%) quartiles (top side). The buffer system displays the shortest tail and a high frequency density around its peak value; the ferrocyanide system displays a long tail with frequencies around its lower bound and a pronounced peak at its modal value; the microalgae system displays an intermediate pattern.

Table 1: Acclimation period statistical analysis for all MFC configurations (all values in V)

System	Mean	SD	Mode	Min	1 <sup>st</sup> Quart.	Median	3 <sup>rd</sup> Quart.	Max
Buffer	0.49891	0.01464	0.518	0.452	0.489	0.499	0.512	0.518
Ferrocyanide	0.48945	0.04741	0.522	0.352	0.486	0.508	0.522	0.522
Microalgae	0.49605	0.02245	0.519	0.423	0.484	0.499	0.519	0.519

Figure 4 displays the full 5 days measurements of potential outputs for all MFC configurations. After its brief peak at 518mV, the buffer system displayed a series of rapid declines into half-day plateaus; the ferrocyanide system went into a rapid decline after its peak of

522mV, sharply dropping to a long plateau around 490mV followed by a steep decline to its lower values; the microalgae system displayed again a more stable intermediate behavior, declining after its initial peak at 519mV into a long plateau around 470mV, followed by gradual declines to lower level plateaus.

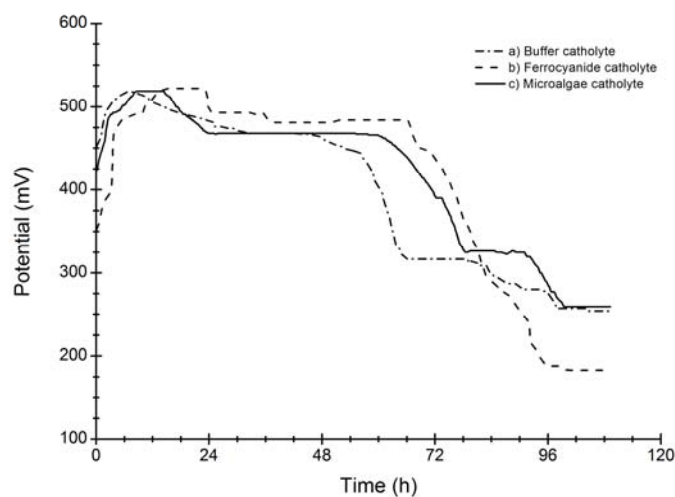
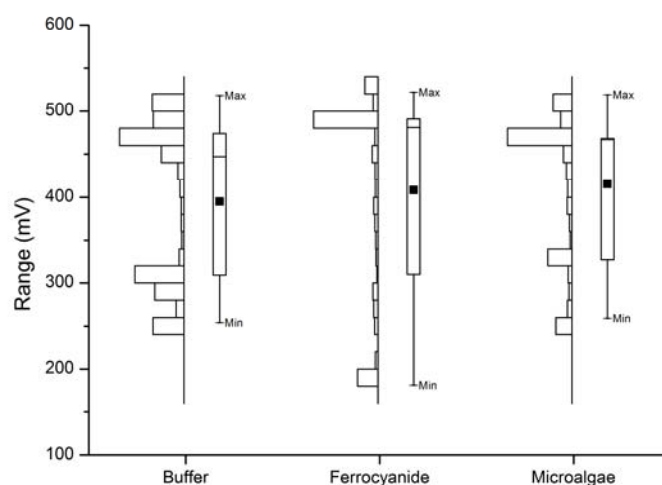


Fig. 4: Potential output for all MFC configurations operated in batch mode. The buffer system (a) displays gradual cascades into half-day plateaus; the ferrocyanide system (b) displays a sharp drop into a mid-level, long-lasting plateau and a general abrupt behavior; the microalgae system (c) displays an intermediate behavior with gradual cascades and a long-lasting mid-level plateau.

Statistical analysis of the full time series offers a clearer image of behavioral patterns (Table 2). Modal values for all systems no longer coincide with their respective maximal values due to the prominence of long-lasting plateaus at lower potential levels; this reflects into lower mean values (mean $\pm$ SD: 0.39494 $\pm$ 0.09382V for the buffer system, 0.40825 $\pm$ 0.11835V for ferrocyanide and 0.4154 $\pm$ 0.08411V for microalgae), which are in turn lower than the respective median values, indicating frequency polarization and long left tails in the frequency distributions. This is more clearly displayed in the corresponding frequency histograms and box plots (Fig. 5): all distributions display a roughly bimodal pattern, with frequencies aggregating towards the lower end of the spectrum - this is more pronounced in the buffer system with its twin plateaus; the ferrocyanide system has the longer tail with a high-value mode and a series of low frequencies over its full range, consistent with its abrupt behavior; the microalgae system displays an intermediate pattern, with high-end and low-end modal plateaus and a shorter tail.

Table 2: Statistical analysis for the 5-day time series for all MFC configurations (all values in V)

System	Mean	SD	Mode	Min	1 <sup>st</sup> Quart.	Median	3 <sup>rd</sup> Quart.	Max
Buffer	0.39494	0.09382	0.317	0.254	0.309	0.447	0.474	0.518
Ferrocyanide	0.40825	0.11835	0.484	0.181	0.310	0.481	0.491	0.522
Microalgae	0.41540	0.08411	0.468	0.259	0.327	0.467	0.468	0.519



*Fig. 5: Box plots and frequency histograms of potential output for all MFC configurations. Solid squares indicate mean values; boxes display 1<sup>st</sup> (25%) quartiles (bottom side), median values (middle line) and 3<sup>rd</sup> (75%) quartiles (top side). The buffer system displays a roughly bimodal behavior with its twin-end plateaus; the ferrocyanide system displays the longer tail and with a high-value mode, indicating its abrupt behavior; the microalgae system displays an intermediate, smoother behavior with more gradual cascades.*

Coulombic efficiencies for all MFC configurations were calculated by integrating the total collected current over time over an external resistance of  $105\Omega$  (Eq. 3, 4). The three systems attained roughly similar coulombic efficiency scores ( $36.0\pm 0.9\%$ ): the buffer system attained the lowest score of 35.1%, the ferrocyanide system 36.3% and the microalgae system attained the highest score of 36.9%, consistent with previously observed low efficiency scores pertaining to glucose oxidation.

### 3.2 Polarization behavior

Figure 6 shows the polarization curves of potential and power density outputs vs. current density for all MFC configurations; polarization curves were obtained by a constant resistance discharge method (i.e. by connecting a gradually decreasing external resistance load to the MFCs and measuring potential and current responses). The buffer catholyte system attained the lowest power density of  $20\text{mW/m}^2$  over a narrow current density range of up to  $155\text{mA/m}^2$ ; the ferrocyanide and microalgae catholyte systems attained the same high power density over a much wider range: up to  $950\text{mA/m}^2$  for ferrocyanide vs. up to  $750\text{mA/m}^2$  for microalgae – for both systems, the highest power density of  $118\pm 1\text{mW/m}^2$  occurred at the  $702\pm 2\text{mA/m}^2$  current density level, corresponding to an external resistance value of  $105\pm 5\Omega$  and a potential output of  $468.5\pm 0.5\text{mV}$ .

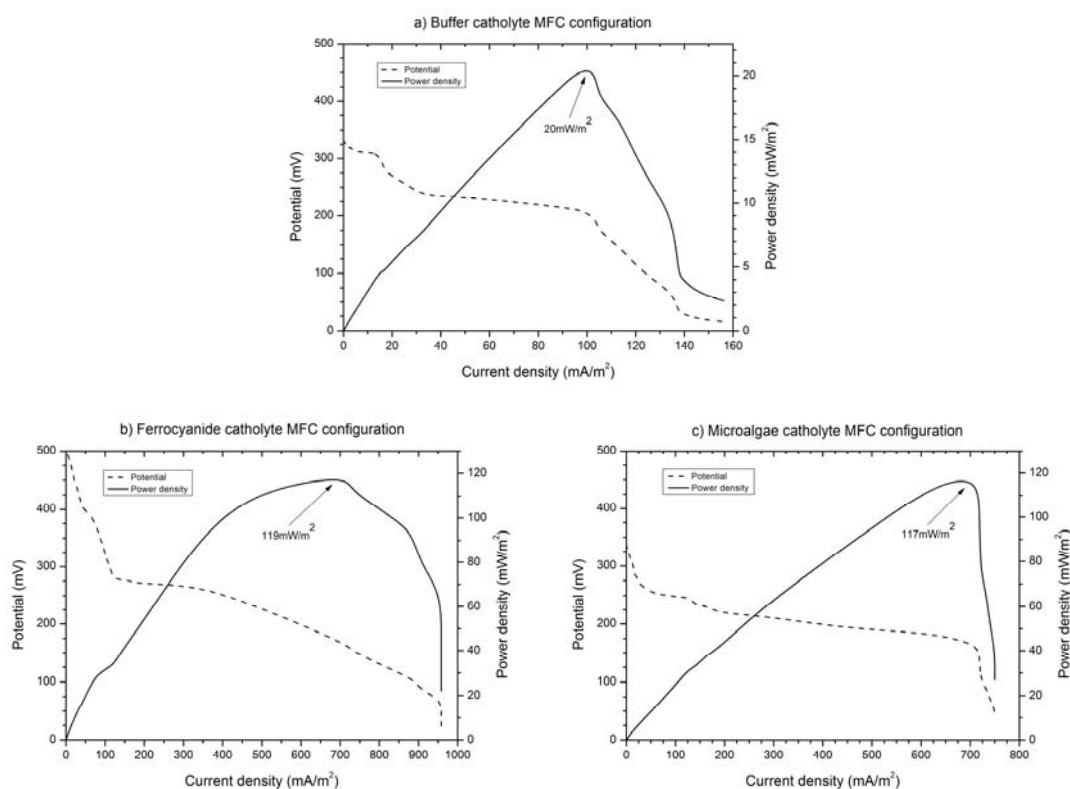


Fig. 6: Polarization graphs for all MFC configurations; the buffer system (a) attained the lowest power density of  $20\text{mW/m}^2$ ; both the ferrocyanide (b) and the microalgae (c) systems attained the highest power density of  $118\pm 1\text{mW/m}^2$  at the  $702\pm 2\text{mA/m}^2$  current density level, corresponding to an external resistance value of  $105\pm 5\Omega$  and a potential output of  $468.5\pm 0.5\text{mV}$ .

### 3.3 Cyclic voltammetry

Cyclic voltammetry measurements were conducted in both chambers to examine the electrochemical behavior of the systems, to determine the double layer capacity of the bioelectrodes and to observe the redox activity in both chambers (Fig. 7). The anode voltammograms reveal the same redox activity for all three systems, displaying two reversible redox signals near pH 6.5: a reversible peak with good intensity at  $-0.465\pm 0.005\text{V}$  vs. SCE, corresponding to the  $\text{NAD}^+/\text{NADH}$  transition ( $E^0$  of  $-0.320\text{V}$  vs. SHE) [2, 10, 11], and a second reversible peak with smaller intensity at  $0.592\pm 0.015\text{V}$  vs. SCE, corresponding to the oxygen reduction potential ( $\text{O}_2/\text{H}_2\text{O}$ :  $E^0$  of  $0.820\text{V}$  vs. SHE).

Cathode voltammograms showed different behavior patterns between systems: the buffer system displayed a single reduction peak at  $0.104\text{V}$  vs. SCE that decreased in value, signifying an irreversible reaction; the ferrocyanide system presented a reversible peak couple at  $0.610\text{V}$  vs. SCE, most possibly attributed to the cathodic oxygen reduction reaction (voltammetry was conducted over the  $0.0$  to  $1.2\text{V}$  range, because at negative potentials the cathode switches to electrolysis); the microalgae system presented a well-defined redox couple at  $0.515\text{V}$  vs. SCE, corresponding to the nitrate reduction potential ( $\text{NO}_3^-/\text{N}_2$ :  $E^0$  of  $0.740\text{V}$  vs. SHE) [2] - another small reduction peak without an identifiable corresponding oxidation peak was observed at  $-0.120\text{V}$  vs. SCE, thus the compound reduction was regarded as permanently reduced.

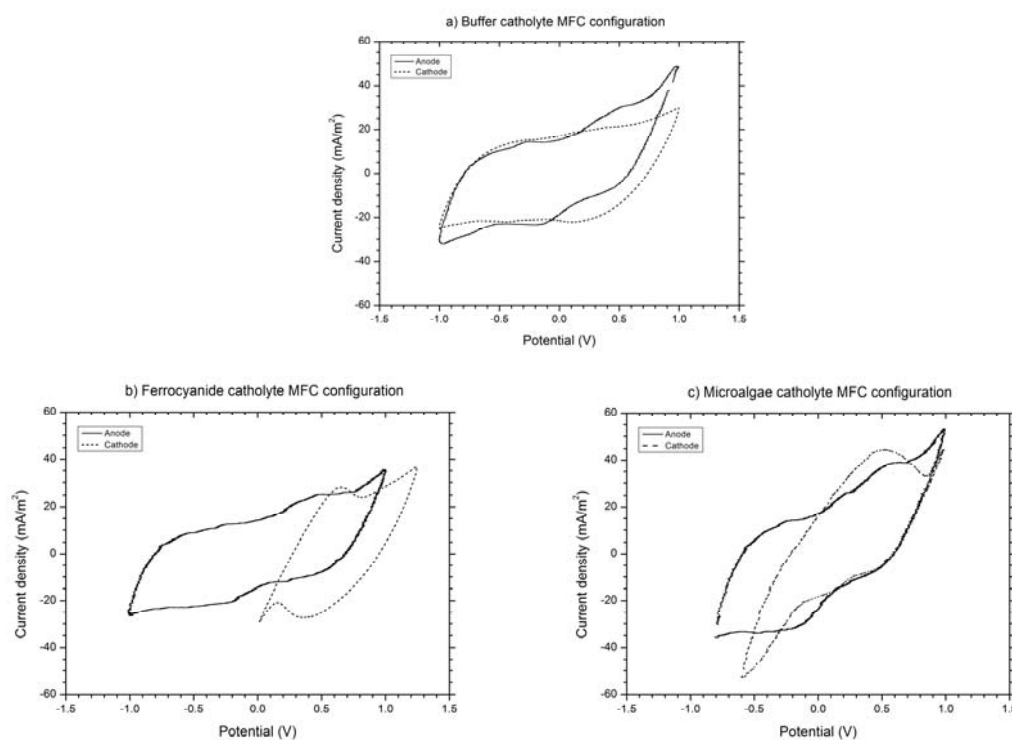


Fig. 7: Cyclic voltammetry (vs. SCE) profiles generated during stabilized phase of MFC operation, displaying anodic and cathodic responses for (a) the buffer catholyte configuration, (b) the ferrocyanide system and (c) the microalgae system. The cathodic profile of system (b) does not extend into the negative potential range, as this initiates electrolysis instead.

Double-layer capacities of the bioelectrodes (Table 3) were calculated from the voltammograms by measuring open circuit potentials and anodic/cathodic currents ( $I_a/I_c$ ), according to the formula:

$$\frac{I_a - I_c}{2} = C_{DL} \frac{dE}{dt} \quad (5)$$

Table 3: Double-layer capacities and generated electrons for all configurations

System	Potential (mV)	DL Capacity ( $\mu\text{F}/\text{cm}^2$ )		$e^-$ generated ( $\mu\text{moles}$ )	
		Anode	Cathode	Anode	Cathode
Buffer	348	1.88	1.85	0.3152	0.3100
Ferrocyanide	487	1.61	1.04	0.3776	0.2439
Microalgae	397	2.26	2.03	0.4321	0.3881

### 3.4 Conductivity, pH and dissolved oxygen

Conductivity (Fig. 8), pH (Fig. 9) and dissolved oxygen (Fig. 10) were monitored in 24-hour intervals for the full 5 days of operation in the electrolytes of both chambers for all MFC configurations.

Anodic conductivities displayed a small decline in all systems within the first two days of operation, followed by a gradual increase afterwards; this is consistent with the acclimation period required by the microbial colonies to reach their maximum potential outputs. Cathodic conductivities remained stable throughout operation for all systems, with the microalgae system

displaying a marked higher conductivity ( $76.85 \pm 0.55 \text{ S/m}^2$ ) vs. the other systems ( $70.8 \pm 0.6 \text{ S/m}^2$  for the buffer system and  $67.6 \pm 0.5 \text{ S/m}^2$  for the ferrocyanide system).

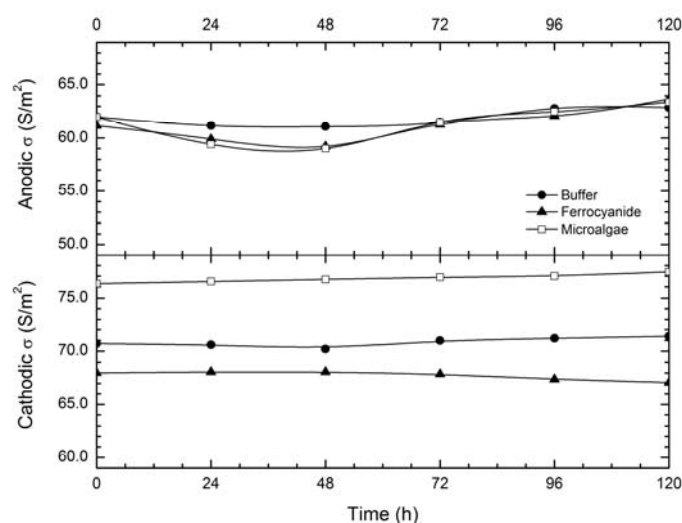


Fig. 8: Conductivity ( $\sigma$ ) profiles for all MFC configurations. Anodic profiles display a small decline within the first two days of operation, attributed to the acclimation period of the microbial colonies. Cathodic profiles remain stable, with a marked higher conductivity presented by the microalgae MFC system.

Anodic pH displayed a similar behavior of gradual decline into the acidic region in all systems – the anolyte of the buffer system restrained this decline in the second day of operation, following the common trend afterwards. Cathodic pH presented a different pattern across systems: the buffer and the microalgae catholytes retained on average a neutral pH throughout operation; the ferrocyanide catholyte started low in the acidic region, displaying a gradual increase afterwards.

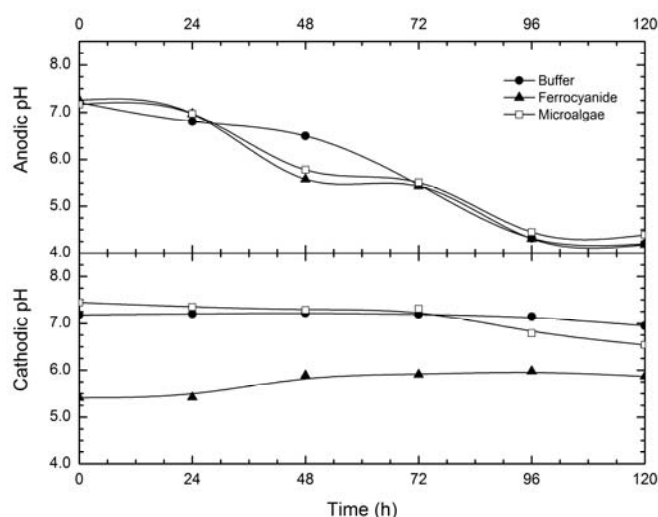


Fig. 9: pH profiles for all MFC configurations. Anodic profiles display a gradual decline into the acidic region; cathodic profiles remain within the neutral pH region for the buffer and the microalgae systems, while the ferrocyanide catholyte remains relatively low in the acidic region.

Anodic DO levels remained within an expected very low range ( $<1.00 \text{ mg/L}$ ) for all systems, due to the anaerobic conditions of the anode chamber – it is not clear if small variations can be safely attributed to chance, although the microalgae system did display a more stable behavior (possibly due to oxygen diffusion through the PEM) compared to the rest, which nearly dropped to zero by the end of the operation period. Cathodic DO levels remained expectedly stable

throughout operation for the microalgae system, due to the constant supply of oxygen by the microalgal respiration – DO levels followed a marked decline in both the buffer and the ferrocyanide systems throughout operation, reaching 48% and 44% drops respectively by the end of the 5-day period. This helps explain the observed instability in generated potentials by the buffer and the ferrocyanide systems (short-lived plateaus and sharp declines respectively) vs. the smoother behavior of the microalgae system.

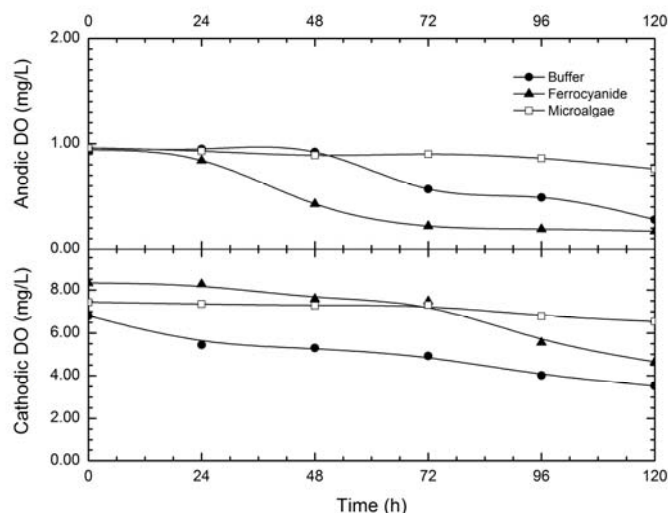


Fig. 10: DO profiles for all MFC configurations. Anodic profiles remain within a low range ( $<1\text{mg/L}$ ); cathodic DO levels for the microalgae catholyte remain within the  $7.00\text{mg/L}$  range throughout operation, while they drop to nearly half their initial value by the end of the operational period for the buffer and the ferrocyanide catholytes, explaining their relative instability in electrochemical performance.

## Conclusions

The present study tested the hypothesis of using microalgae as native oxygen suppliers in bicameral MFC configurations, to combine oxygen production by microalgal photosynthesis in the cathode and removal of pollutants in the anode. We have assembled an MFC experimental prototype that employs a *Saccharomyces cerevisiae* monoculture in the bioanode (using glucose and maltose solutions as substrate) and cultures of microalgae in the cathode to counter oxygen depletion in the catholyte, aiming to improve MFC power performance by stabilizing DO levels. This prototype was tested against two other configurations that retained the same microbial bioanode, but employed different catholytes: a phosphate buffer used as a low benchmark and a potassium ferrocyanide mediator solution; their performance was compared in terms of electrochemical response, power production and coulombic efficiency.

Data analysis revealed that the ferrocyanide and the microalgae systems presented comparable electrochemical responses, reaching power densities of  $\sim 118\text{mW/m}^2$  around the current density level of  $700\text{mA/m}^2$  and similar maxima in generated potentials ( $\sim 520\text{mV}$ ) – the buffer benchmark performance has been expectedly low. However, the microalgae system presented a more stable electrochemical response over time (with faster acclimation times, smoother transitions into lower production levels and a higher average performance throughout the full operation time), benefitting from the constant oxygen supply provided by microalgal photosynthesis at the cathode. Coulombic efficiencies have been similarly higher ( $\sim 37\%$ ) for the microalgae system, as well as double layer capacities for both its bioelectrodes ( $2.26$  to  $2.03\mu\text{F/cm}^2$ ), which indicate satisfactory electrochemical activity of the associated biofilms. Lastly, DO levels in the catholyte have remained relatively constant throughout operation, in contrast to the other systems that dropped to nearly half their initial values at the end.

Overall, microalgae biocathodes in MFC systems compensate oxygen depletion in the cathode by photosynthetic oxygen production, thus they alleviate the energy input demand for aeration; they also provide a comparable alternative to chemical mediators, thus negating the cost of mediator replenishment, and present an environment-friendly solution due to their zero toxicity. The above provide reasonable ground to suggest coupling microalgae MFCs to wastewater treatment processes as cost-effective, sustainable and power-efficient solutions.

### Acknowledgements

This work was supported by the Sectorial Operational Program for Human Resources Development 2007-2013, co-financed by the European Social Fund under project numbers POSDRU/107/1.5/S/80765, POSDRU/107/1.5/S/82514 and IDEI PN-II-ID-PCE-2011-3-0815 (UEFISCDI).

### References

- [1] Z. He and L. T. Angenent, "Application of bacterial biocathodes in microbial fuel cells", *Electroanalysis* **18**:19-20 (2006).
- [2] P. Aelterman, K. Rabaey, T.H. Pham, N. Boon and W. Verstraete, "Continuous electricity generation at high voltages and currents using stacked microbial fuel cells"; *Environ. Sci. Technol.* **40**:3388-3394 (2006).
- [3] P. T. Hai, J. K. Jang, S. Chang, and B. H. Kim, "Improvement of cathode reaction of a mediatorless microbial fuel cell", *J. Microbiol. Biotechnol.* **14**(2):324–329 (2004).
- [4] D. R. Lide, *Handbook of Chemistry and Physics*, Ed. CRC Press, FL, 2000-2001.
- [5] F. Zhao, F. Harnisch, U. Schroder, F. Scholz, P. Bogdanoff and I. Herrmann, "Challenges and constraints of using oxygen cathodes in microbial fuel cells", *Environ. Sci. Technol.* **40**(17):5193-5199 (2006).
- [6] K. Rabaey, P. Clauwaert, P. Aelterman and W. Verstraete, "Tubular microbial fuel cells for efficient electricity generation", *Environ. Sci. Technol.* **39**:8077-8082 (2005).
- [7] M. Rahimnejad, G. D. Najafpour, A. A. Ghoreyshi, M. Shakeri and H. Zare, "Methylene blue as electron promoters in microbial fuel cell", *Int. J. Hydrogen Energy* **36**:13335-13341 (2011).
- [8] L. Huang, J. M. Regan, and X. Quan, "Electron transfer mechanisms, new applications, and performance of biocathode microbial fuel cells", *Bioresour. Technol.* **102**(1):316–23 (2011).
- [9] B. Erable, I. Vandecastelaere, M. Faimali, M. L. Delia, L. Etcheverry, P. Vandamme and A. Bergel, "Marine aerobic biofilm as biocathode catalyst", *Bioelectrochemistry* **78**:51-56 (2010).
- [10] X. Xia, J. C. Tokash, F. Zhang, P. Liang, X. Huang and B. E. Logan, "Oxygen-reducing biocathodes operating with passive oxygen transfer in microbial fuel cells", *Environ. Sci. Technol.* **47**(4):2085–2091 (2013).
- [11] M. Rosenbaum, F. Aulenta, M. Villano and L. T. Angenent, "Cathodes as electron donors for microbial metabolism: which extracellular electron transfer mechanisms are involved?", *Bioresour. Technol.* **102**:324–333 (2011).
- [12] O. Perez-Garcia, F. M. Escalante, L. E. de Bashan and Y. Bashan, "Review - Heterotrophic cultures of microalgae: metabolism and potential products", *Water Res.* **45**:11-36 (2011).
- [13] E. T. Sayed, T. Tsujiguchi and N. Nakagawa, "Catalytic activity of baker's yeast in a mediatorless microbial fuel cell", *Bioelectrochemistry* **86**:97–101 (2012).
- [14] M. Rahimnejad, A. A. Ghoreyshi, G. D. Najafpour, H. Younesi and M. Shakeri, "A novel microbial fuel cell stack for continuous production of clean energy", *Int. J. Hydrogen Energy* **37**:5992-6000 (2012).
- [15] C. G. Liu, C. Xue, Y. H. Lin and F. W. Bai, "Research review paper: Redox potential control and applications in microaerobic and anaerobic fermentations", *Biotechnol. Adv.* **31**:257–265 (2013).
- [16] B. E. Logan, *Microbial Fuel Cells*, John Wiley & Sons, Inc., Hoboken, NJ, (2008).
- [17] S. Oh, B. Min and B. E. Logan, "Cathode performance as a factor in electricity generation in microbial fuel cells", *Environ. Sci. Technol.* **38**:4900-4904 (2004).